MedCrave
Step into the World of Research
International Journal of Petrochemical Science & Engineering

Research Article

Open Access
CrossMark

A new approach for determination of adsorption energy for each adsorption site and improve conventional adsorption isotherms

Abstract

In the present study, a new approach for determination of energy distribution (ED) of heterogeneous solid adsorbents is presented. This approach implements pore size distribution (PSD) data of a porous adsorbent obtained from adsorption measurements to estimate the ED of the solid. Moreover, the proposed algorithm imposes some modifications on the conventional adsorption models to improve them and provide better prediction of adsorption behavior. Adsorption data of four different heterogeneous cases were used to evaluate the proposed algorithm. From the results, the proposed algorithm provided better estimation of adsorption isotherm than conventional adsorption models such as Unilan, Toth and Sips as well as easily calculated ED. The accuracy of the proposed algorithm is greatly depends on selection of appropriate PSD determination method. The proposed algorithm regarded as a trustworthy procedure for reliable estimation of ED of heterogeneous solid adsorbents.

Keywords: energy distribution, adsorption isotherme, Kelvin, SHN1, PSD

Volume 3 Issue 4 - 2018

Mehrzad Arjmandi,[1] Ali Ahmadpour,[1] Abolfazl Arjmandi[2]

[1]Department of Chemical Engineering, Ferdowsi University of Mashhad, Iran

[2]Department of Chemical Engineering, Mazandaran University of Science and Technology, Iran

Correspondence: Mehrzad Arjmandi, Department of Chemical Engineering, Faculty of Engineering, Ferdowsi University of Mashhad, Mashhad, Iran, Tel 009891121089990, Email mehrzad.arjmandi89@gmail.com

Received: March 08, 2018 | **Published:** September 10, 2018

Introduction

Adsorption is a surface phenomenon that one or more substances which are originally presented in a fluid phase would remove from that phase by accumulation at the interface between the fluid and a solid surface. Adsorption mechanisms are typically classified as physical, chemical and electrostatic adsorption, in which for the gas separation systems, the physical adsorption is only considered. In the case of physical adsorption, weak intermolecular forces such as van der Waals provide the required driving force of the process.[1] Generally, physical adsorption data is used to describe the main characteristics of the solid surfaces.[2,3] The adsorption that occurs on different sites of the solid surface follows the adsorption isotherms.[4] The early presented models for prediction of gas adsorption on a solid surface assumed the surface to be uniform and homogeneous. The first quantitative model was discussed by Langmuir assuming monolayer coverage.[6]

Brunner, Emmett and Teller (BET) proposed an adsorption isotherm with multilayer adsorption on the solid surface.[6] Both Langmuir and BET isotherms are based on kinetic mechanisms and assume adsorption occurring on fixed sites of the surface with no lateral interactions among adsorbed molecules. Such isotherms could be applied reliably for solids with uniform pores. However, porous media include pores with different sizes and this pore size distribution can severely affect the adsorption characteristics and surface area of the sorbent.[7,8] Since pores with various sizes, have different energies, one of the greatest problems of physical adsorption is the precise description of the heterogeneity of the adsorbent. Many investigators working in the field of physical adsorption have devoted their researches to this problem,[9] but the issue of heterogeneity is still one of the great unresolved problems in this field. Accurate estimation of energy distribution and/or pore size distribution of non homogeneous adsorption systems is considered as an important design and operational consideration.[10] Adsorption measurement on each solid site with identified energy is an impractical process; as a result, relatively complex theories are applied in many cases for estimation of such distributions.[11]

There have been several researches regarding determination of energy distribution (ED) for heterogeneous adsorbents.[12–15] In 1987, Tarazona[13] applied Density Functional Theory (DFT) to the adsorption isotherms. Merz[14] used the regularization technique along with the generalized cross-validation (GCV) for estimation of ED using Langmuir and BET isotherms. House[15] applied the second order penalized least square (PLS) for the prediction of ED in heterogeneous solid adsorbents. Duda[16] investigated ED of microporous systems using multivariate identification. Various models have been proposed for estimation of pore size distribution (PSD)[17–27]and ED[14–16,25,28–32]for solid adsorbents. However, by estimating an ED by one of these methods, the conventional isotherms with constant adsorption energy could not be reliably applied. In other words, by even applying an identified ED function, it is impossible to obtain related energy for all solid pores individually and adsorption measurement on such pores with different energies is impractical.

In this study, a new algorithm (called M.A.A algorithm) is presented for determination of ED of heterogeneous solid adsorbents. In this algorithm, the PSD of adsorbent is first determined by the method proposed by Shahsavand[26], and then by considering some assumptions (that are discussed in the theory section) and following the presented algorithm, the ED would be determined. The advantage of the proposed algorithm is that by following such procedure it is possible to evaluate an energy related to solid pores and subsequently determine the amount adsorbed on each solid site with the identified energy. The success of this algorithm is greatly depends on choosing an accurate method for the estimation of PSD of solid adsorbent in addition to maximum and minimum of surface energy that is usually predetermined values or could be determined by doing a few and simple experiments.

Adsorption Isotherms

As mentioned before, adsorption occurs on the surface of a solid and follows the adsorption isotherms.[4] A wide variety of equilibrium isotherm models such as Langmuir, Freundlich, BET, Redlich-Peterson, Dubinin-Radushkevich, Temkin, Toth, Koble-Corrigan, Sips, Khan, Hill, Flory-Huggins and Radke-Prausnitz have been proposed by many researchers based on three different approaches including kinetic, thermodynamic and potential.[33] Based on the kinetic approach, adsorption equilibrium is defined a situation in which the adsorption and desorption rates are equal.[5–34] The thermodynamics provide framework for deriving numerous forms of adsorption isotherm models as the second approach.[12–35] The potential theory, as the third approach, usually conveys the main idea in the generation of characteristic curve.[36]

Generally, adsorption isotherms could be classified into three categories of two parametric isotherms (e.g. Langmuir, Freundlich, Dubinin–Radushkevich, Temkin, Flory-Huggin, Volmer and Hill), three parametric isotherms (e.g. Redlich–Peterson, Sips, Toth, Unilan, Koble–Corrigan, Khan, Radke-Prausnitz, Fowler-Guggenhein and Hill-deBoer), and multilayer adsorption (BET).[4] In order to investigate improvement of conventional adsorption isotherms by using the proposed algorithm, three widely used isotherms of Sips, Toth and Unilan were evaluated among various adsorption isotherm models due to the it simplicity as well as having the desired accuracy.

Sips isotherm

The Sips isotherm is a combination of Freundlich and Langmuir models that is used for adsorption systems with heterogeneous surfaces. Unlike Freundlich isotherm[37] that does not provide accurate estimation at high levels of pressure, the Sips model predicts accurate estimation even at high pressures. However, both models do not satisfy the Henry's law[38] at very low pressures. The Sips isotherm is described as:

$$C_\mu = C_{\mu s}\frac{(bP)^{1/n}}{1+(bP)^{1/n}} \tag{1}$$

$$b = b_\infty \exp\left(\frac{Q}{RT}\right) \tag{2}$$

Where, P denotes the adsorption pressure, Cμ is the amount adsorbed, Cμs maximum amount adsorbed at adsorption temperature of T, and b is the adsorption affinity at infinite temperature and n is a constant parameter. As it seen from the above equations, the Sips model is similar to the Langmuir isotherm; however the only difference between them is addition of parameter ''n'' in the Sips model which is a measure of the heterogeneity nature of the adsorbent surface with n=1 for the homogeneous surfaces.[1]

Toth isotherm

Unlike Sips model that does not satisfy the low pressure limit, the Toth isotherm is capable of satisfying both high and low pressure limits as well as the Henry's law.[1,39] This equation describes well many systems with sub-monolayer coverage. The Toth isotherm is described by the following equation:

$$C_\mu = C_{\mu s}\frac{bp}{\left[1+(bp)^t\right]^{1/t}} \tag{3}$$

$$b = b_\infty \exp\left(\frac{Q}{RT}\right) \tag{4}$$

Where t is a constant parameter

Unilan isotherm

The Unilan equation is another empirical relation that obtained by assuming a patch wise topography on the solid surface and each patch is ideal such that the local Langmuir isotherm is applicable over each patch. The Unilan equation provides well behaviors at low and high pressures. This isotherm is described as:

$$C_\mu = \frac{c_{\mu s}}{2s}\ln\left(\frac{1+\bar{b}.\exp(s)P}{1+\bar{b}.\exp(-s)P}\right) \tag{5}$$

$$\bar{b} = b_\infty \exp\left(\frac{\bar{E}}{RT}\right) \tag{6}$$

$$\bar{E} = \frac{E_{\max}+E_{\min}}{2} \tag{7}$$

$$s = \frac{E_{\max}-E_{\min}}{2RT} \tag{8}$$

Where E_{max} and E_{min} are maximum and minimum energies of distribution and $\bar{b}$ is the adsorption affinity at infinite temperature. The parameter ''s'' characterizes the heterogeneity of the system.

Theory

Physical adsorption on heterogeneous surfaces could be described by Fredholm integral equation. In general, the Fredholm integral equation of the first kind is characterized by the following definite integral:[40–42]

$$g(t) = \int_a^b K(t,s)F(s)\,ds \tag{9}$$

In which, F(s) is an unknown distribution function that should be determined and K(t,s) is kernel (isotherm) of the equation that would be chosen based on the adsorbent, adsorbates, pressure and temperature of an adsorption process. It is assumed that the adjacent adsorption sites do not have any energy interferences. It can described, with a good approximation, the relation between the amounts adsorbed on any sites of the solid with particular energy, adsorption pressure and temperature using the Langmuir equation. This integral equation could be safely applied for the determination of PSD and ED of an adsorbent as follows:

$$g(P_i) = \int_{r_{\min}}^{\infty} g(e,P_i,T)F(r)dr \tag{10}$$

$$g(P_i) = \int_{e_{\min}}^{e_{\max}} g(e,P_i,T)F(e)\,de \tag{11}$$

From this equation, it is clear that having the amount adsorbed on the adsorbent at constant temperature and different pressures as well as adsorption isotherm and integral limits; it can easily compute PSD and ED of the porous solid. However, calculation of ED in

most cases is usually done by determining the most frequent energy within the adsorbent assuming this constant and uniform energy for the solid surface and considering the energy as a known parameter of the adsorption isotherm. This assumption has high accuracy for homogeneous adsorbents; but by increasing heterogeneity of the surfaces the accuracy is reduced. On this basis, the related energy of any adsorption pressure should be determined.

As a new approach for determination of ED of a solid adsorbent presented here, it is necessary to determine the PSD of the solid in advance. As it is shown in Eq. (4), constant parameter of total energy of solid is used for the calculation of affinity coefficient ''b''. Since all this parameters are fixed, the parameter ''b'' is considered constant. In reality, parameter ''b'' is not constant within the system and should be determined for each adsorption site. For calculating this parameter for each site on the solid, the related energy should be determined beforehand. With respect to Eq. (6), the maximum and minimum energy of adsorption could be determined experimentally and average of these values could be considered as adsorption energy in the Unilan equation. This procedure is applied for different isotherms. It should be noted that we aimed to determine corresponding adsorption energy for each adsorption site. In other words, at each pressure the energy of the adsorbent should be defined. On this basis, parameters Q, E and b in the isotherm models should not be considered constants and only function of adsorption pressure. The proposed procedure is shown in Figure 1.

Figure 1 Flow chart of direct route calculation of E_i and b_i for each P_i.

In order to follow the procedure depicted in Figure 1, ED equation should be known. However, various conventional methods of computing ED could not follow the presented procedure. That is why we need to follow a different path where the required information is available. Here, we introduce an indirect path for computing E_i and b_i at each operational pressure that is presented on Figure 2.

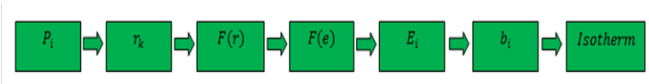

Figure 2 Proposed flow chart of indirect route calculation of E_i and b_i for each P_i.

The proposed algorithm (M.A.A) with the priori assumptions are described below:

1. In the first step, by using one of the conventional methods of PSD determination of porous solids, the PSD of adsorbent is determined.
2. Then, using the experimental or theoretical information about maximum and minimum effective pore radius in adsorbent, the radius limits would be corrected. For example, among radius obtained from the Kelvin equation, most of them may relates to small radiuses and a small portion of them corresponds to large radiuses. In such situation, the maximum energy would be considered for the largest radius and all others would be regarded as effective pore radius. In other words, we try to reduce the errors in computing PSD of solids in this step.
3. After determination of PSD of adsorbent with the corrected limits, a Gaussian function is fitted to the PSD data in order to obtain a function for this distribution.
4. Now, using the following equation, the range of minimum and maximum effective pore radius is divided into ''n'' intervals as follows:

$$dr = \lim_{n\to\infty}\left(\frac{\left|r_{\max} - r_{\min}\right|}{n}\right) \tag{12}$$

Do the same procedure to the step 4 for determination of de with respect to maximum and minimum energy of the solid.

$$de = \lim_{n\to\infty}\left(\frac{\left|E_{\max} - E_{\min}\right|}{n}\right) \tag{13}$$

Using the following equation (Do 1998), the ED would be determined from the PSD function obtained in step 3.

$$f\left(e\right) = f\left(r\right).\frac{dr}{de} \tag{14}$$

In this equation, it is assumed that energy in the pores depends only on the radius of the pore and other factors do not affect it. In other words, the shape of energy distribution function is similar to the PSD ones.The main goal is to relate energy of each pore to the adsorption pressure. In step 6, relationships between pressure and energy have presented and now must establish a relationship between the pore radius and pressure. Therefore, we should obtain a radius corresponds to the condensation or evaporation pressure using Kelvin equation.[34]

$$r_k\left(P_i\right) = \frac{\sigma\cos\theta\vartheta_M}{RT\ln\left(\frac{P_o}{P_i}\right)} \tag{15}$$

$$r_k\left(P_i\right) = \frac{2\sigma\cos\theta\vartheta_M}{RT\ln\left(\frac{P_o}{P_i}\right)} \tag{16}$$

Where, the threshold radius rk for both condensation and evaporation cases can be computed from the Kelvin equation, respectively. In these equations, σ denotes surface tension, vM molar volume of liquid and P0 vapor pressure of the bulk phase. Kelvin equation is the only model that provides a relation between pressure and pore radius which is used for N2 adsorption data.

1. Now for each rk, calculate an f(r) value using the obtained f(r) function.
2. In this step, calculate f(e) for each f(r) value from step 8.
3. Using f(e) values obtained in step 9 and with respect to the ED function obtained in step 6 and applying inverse theory, energy related to each f(e) value could be determined.
4. b_i values could be determined by applying Eqs. (4) and (6). Substituting b_i values in the adsorption isotherm models provide an accurate isotherm model for prediction of adsorption on heterogeneous solids.
5. Although, the assumption considered in calculating ED of adsor-

bent affect unfavorably the accuracy of the model, the precision of the method in PSD determination has a main role in accurate solution of the proposed algorithm. The summary of the proposed algorithm is presented in (Figure 3).

The PSD of solids investigated in this study are determined by a linear regularization method[43–46] provided by Shahsavand[27] They have provided an accurate and reliable method for correct estimation of PSD for the porous solids from nitrogen adsorption data using Eq. (11).

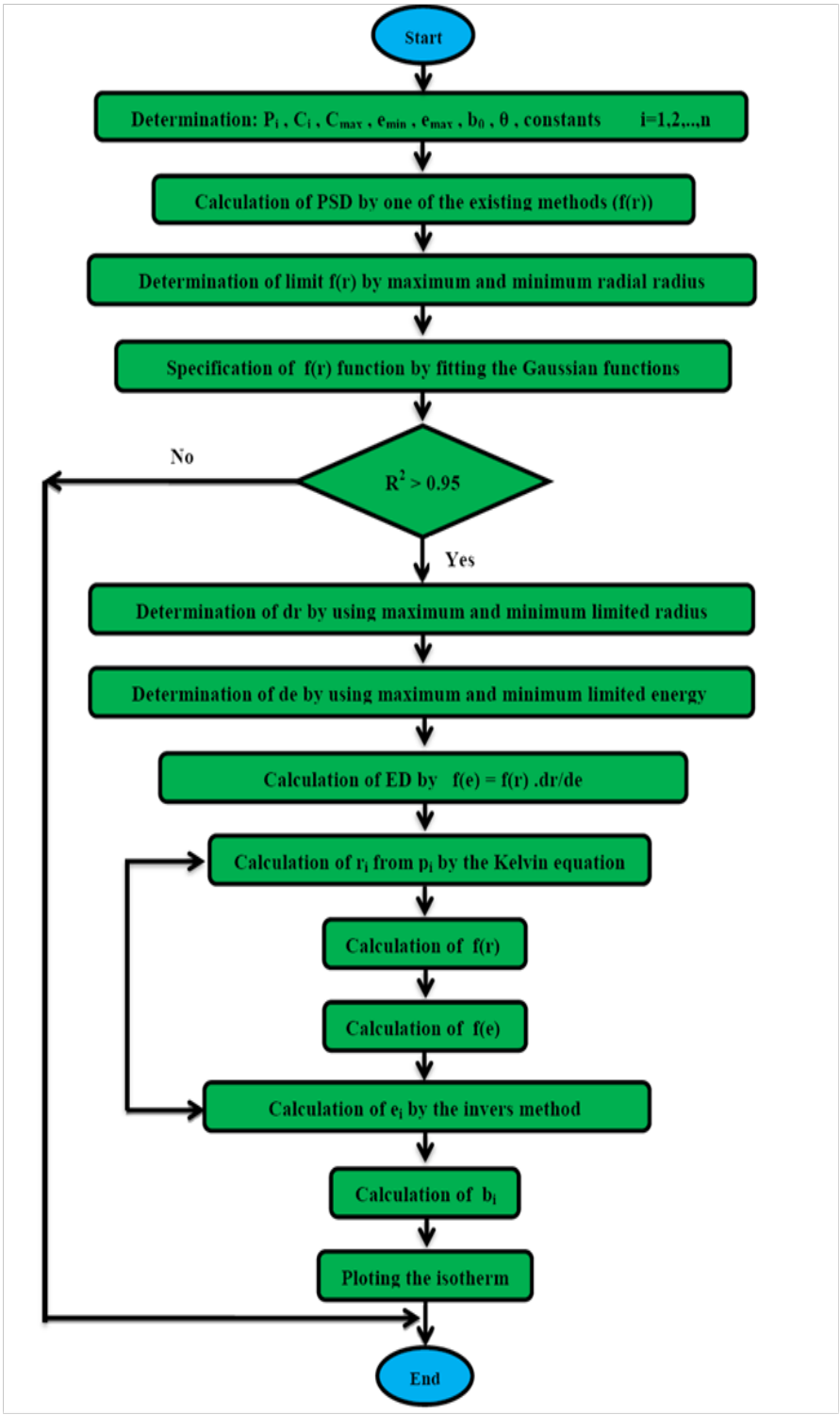

Figure 3 Flow chart of the proposed algorithm

Results and discussion

Four different cases were used to evaluate the proposed algorithm. Usually, studies of surface properties pore size, pore volume and chemical composition of the available surface is done using nitrogen adsorption at liquid N2 temperature of 77K.[47] For this reason, N2 adsorption data of four different adsorbents were used to evaluate the proposed algorithm. The maximum energy of these adsorbents was obtained from the experimental data using regression method and they are presented in Table 1. Moreover, the PSD of each solid was determined using the first order linear regularization method. Using any other method to calculate PSD with sufficient accuracy is also allowed. In each case, three isotherms of Unilan, Sips and Toth are used with some modifications by the proposed algorithm and plotted to evaluate their improvement.

Table 1 The maximum energy considered for different adsorbents (case 1-4)

E_{max} (KJ/mol)	Adsorbate	Adsorbent	NO.
9≈	N_2	CPG 69	**Case 1**
4≈	N_2	NS-$ZnCl_2$	**Case 2**
10≈	N_2	Coal-KOH	**Case 3**
12≈	N_2	NS-KOH	**Case 4**

Case study 1

The adsorption data of Controlled pore glass (CPG-69) heterogeneous adsorbent was used as the first case study. CPG is produced from a special alkali-borosilicate material which is heated above the annealing point but below the temperature that would cause deformation. During this heat operation, two continuous closely intermingled glassy phases are produced. One phase is rich in alkali and boric oxide and is easily soluble in acids and another phase is rich in silica and is insoluble. The borate and alkali phase is washed out by acid solutions at high temperatures followed by a treatment with sodium hydroxide and by washing with water.[48]According to the proposed algorithm, the PSD of solid was determined using linear regularization method and a Gaussian function was fitted to the PSD data, subsequently (Figure 4). Then, using step.(8) and value of maximum energy of adsorption (Table 1), the ED was calculated from the PSD data (Figure 5). After obtaining energy distribution within the solid, the related energy at each operation pressure was determined using the proposed algorithm by using the calculated energy data, the Unilan, Toth and Sips isotherms are plotted against the experimental data in Figure 6. Due to the heterogeneous nature of adsorbent, adsorption isotherms show good behavior and are well able to predict the experimental data. A comparison between the conventional Unilan and Sips isotherms with their modifications by the proposed algorithm was done and the results are presented in Figure 7. From this figure, it is clear that the proposed algorithm improved the adsorption isotherms significantly. If the conventional isotherms are used for the heterogeneous solid adsorption systems, there would be significant errors in predict the adsorption isotherms (Figure 7). In order to better compare the accuracy of the proposed algorithm, the isotherm data points predicted by both modified and conventional Unilan and Sips models are presented in Table 2.

Case study 2

The second case study implemented the N2 adsorption data of a heterogeneous adsorbent prepared from macadamia-nutshell chemically activated with ZnCl2 chemical to nutshell ratio 5% namely NS-ZnCl2.[49] Doing the same procedure as in Case 1, the PSD of the solid was obtained using linear regularization and a Gaussian function was fitted to the PSD data points (Figure 8). Using step (8) and maximum adsorption energy for this heterogeneous adsorbent (presented in Table 1), the ED of this solid was obtained from the PSD data (Figure 9). Similar to the Case Study-1, energy related to each adsorption pressure was obtained using the algorithm proposed in this study. Using the calculated energy data, the Unilan, Sips and Toth modified adsorption isotherms are obtained and the results are compared with the experimental data in Figure 10.

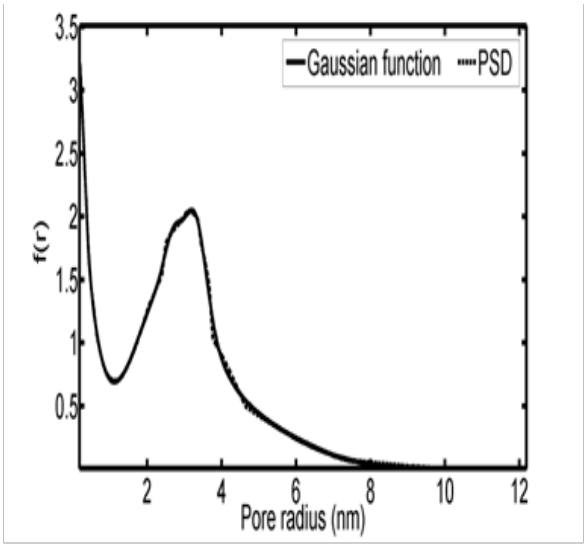

Figure 4 Gaussian function was fitted to the PSD data.

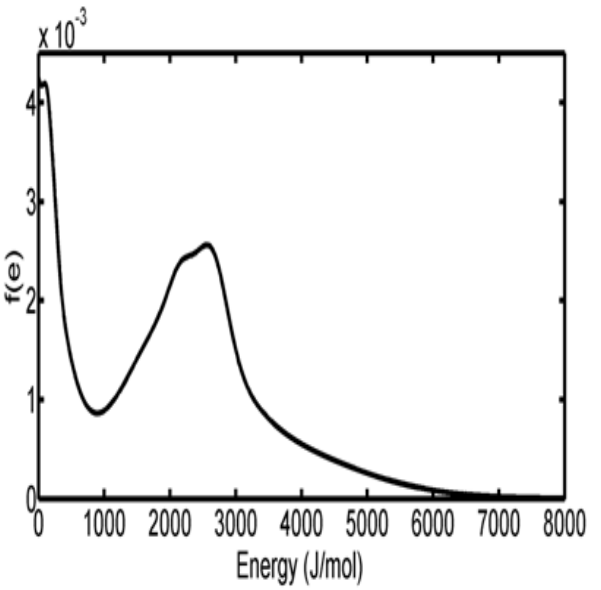

Figure 5 ED was calculated from the PSD data.

Case studies 3&4

In the third and fourth case studies, we have used N2 adsorption data of a macadamia nutshell and a coal based chemically activated

carbons by KOH, respectively.[50] Physical properties of these two activated carbons are presented in Table 3. Following the same procedure, the PSD of solids were obtained using linear regularization and a Gaussian function was fitted to the PSD data to obtain a Gaussian PSD function (Figure 11). The ED of solids is shown in Figure 12. Similar to the previous case Studies, energy related to each adsorption pressure was obtained using the proposed algorithm. Using the calculated energy data,[51,52] modified adsorption isotherms are obtained and the results are compared with the experimental data in Figure 13 (Table 4) (Table 5).

Table 2 Comparison of isotherms data; Sips;Sips-M.A.A & Unilan; Unilan- M.A.A (C: Nitrogen adsorbed)

C_i(Sips) (cm^3/g)	C_i(Sips- M.A.A) (cm^3/g)	C_i(Unilan) (cm^3/g)	C_i(Unilan M.A.A) (cm^3/g)	C_i(Exp.) (cm^3/g)	E_i (J/mol)	P/P_0	No
0	0	0	0	0	0	0	**1**
6.131	0.618	4.831	0.507	0.794	145.0	0.070	**2**
6.379	0.724	5.058	0.651	0.980	163.0	0.098	**3**
6.554	0.837	5.260	0.807	1.086	188.0	0.133	**4**
6.671	0.950	5.427	0.961	1.129	218.0	0.172	**5**
6.733	1.031	5.533	1.068	1.206	239.0	0.203	**6**
6.780	1.108	5.622	1.168	1.237	262.0	0.234	**7**
6.823	1.200	5.717	1.284	1.280	291.0	0.273	**8**
6.848	1.270	5.776	1.370	1.282	320.0	0.301	**9**
6.871	1.336	5.834	1.449	1.405	340.0	0.332	**10**
6.899	1.451	5.914	1.584	1.397	390.0	0.381	**11**
6.925	1.589	5.992	1.739	1.539	457.0	0.437	**12**
6.938	1.689	6.039	1.848	1.582	510.0	0.457	**13**
6.954	1.794	6.096	1.959	1.603	550.0	0.528	**14**
6.965	1.875	6.137	2.042	1.721	580.0	0.570	**15**
6.975	1.972	6.180	2.139	1.805	620.0	0.619	**16**
6.986	2.085	6.216	2.250	1.907	680.0	0.664	**17**
6.988	2.148	6.237	2.310	2.001	710.0	0.692	**18**
6.992	2.206	6.254	2.365	2.066	740.0	0.716	**19**
6.996	2.257	6.272	2.413	2.160	760.0	0.744	**20**
6.999	2.352	6.288	2.500	2.317	820.0	0.769	**21**
7.002	2.470	6.303	2.607	2.520	900.0	0.793	**22**
7.005	2.745	6.320	2.848	2.798	1100	0.821	**23**
7.007	3.008	6.324	3.072	3.131	1300	0.828	**24**
7.008	3.694	6.337	3.638	3.702	1800	0.852	**25**
7.009	4.356	6.341	4.190	4.358	2300	0.859	**26**
7.010	4.795	6.346	4.577	4.767	2650	0.869	**27**
7.011	5.398	6.348	5.161	5.394	3200	0.872	**28**
7.011	6.033	6.352	5.892	6.095	3940	0.879	**29**
7.012	6.610	6.353	6.667	6.538	5010	0.882	**30**
7.014	7.072	6.364	7.086	6.988	7400	0.903	**31**
7.017	7.109	6.381	7.095	7.002	8000	0.938	**32**
7.020	7.115	6.396	7.096	7.033	8100	0.969	**33**
7.022	7.144	6.409	7.099	7.173	9000	0.997	**34**

Table 3 Physical characteristics of two chemically activated carbons

Sample	T (K)	Activation time (min)	Weight loss (%)	Density (g/cm^3)	S_{BET} (m^2/g)	V_{mi} (cm^3/g)	V_{meso} (cm^3/g)	$X_{0,DS}$[†] (nm)
Coal:KOH	973	120	26	0.65	850	0.388	0.046	0.57
NS:KOH	973	60	75	0.29	1075	0.479	0.034	0.63

Table 4 Calculated of energy at each pressure in different cases by algorithm M.A.A

Case 4			Case 3			Case 2			Case 1			
E_i (J/mol)	C_μ (cm^3/g)	P/P_0	E_i (J/mol)	C_μ (cm^3/g)	P/P_0	E_i (J/mol)	C_μ (cm^3/g)	P/P_0	E_i (J/mol)	C_μ (cm^3/g)	P/P_0	NO.
0	0	0	0	0	0	0	0	0	0	0	0	**1**
3.8500	58.884	0.0000	6.2400	37.153	0.0000	14.400	498.20	0.0600	145.00	0.7940	0.0700	**2**
4.1600	77.625	0.0000	6.8000	52.481	0.0000	16.600	551.30	0.0900	163.00	0.9800	0.0980	**3**
4.4600	95.499	0.0001	7.1840	63.000	0.0000	18.900	586.60	0.1200	188.00	1.0860	0.1330	**4**
4.6200	107.15	0.0001	7.5400	72.443	0.0001	21.200	616.10	0.1500	218.00	1.1290	0.1720	**5**
4.8000	120.23	0.0001	8.2000	93.325	0.0001	22.700	636.70	0.1600	239.00	1.2060	0.2030	**6**
5.3000	147.91	0.0003	8.8700	109.65	0.0003	32.100	775.30	0.2900	262.00	1.2370	0.2340	**7**
5.8000	173.78	0.0005	9.7800	130.00	0.0006	38.000	843.10	0.3500	291.00	1.2800	0.2730	**8**
6.5000	194.98	0.0012	10.800	145.00	0.0013	49.000	946.30	0.4400	320.00	1.2820	0.3010	**9**
805.00	234.42	0.0043	12.700	173.78	0.0036	69.800	1040.6	0.5600	340.00	1.4050	0.3320	**10**
9.4000	266.01	0.0097	15.500	194.98	0.0096	161.00	1140.8	0.7800	390.00	1.3970	0.3810	**11**
12.560	283.83	0.0297	20.300	208.93	0.0292	229.00	1149.7	0.8400	457.00	1.5390	0.4370	**12**
16.000	294.84	0.0632	25.700	224.87	0.0611	426.30	1164.4	0.9100	510.00	1.5820	0.4750	**13**
18.000	298.62	0.0850	29.200	227.84	0.0853	649.40	1167.3	0.9400	550.00	1.6030	0.5280	**14**
19.550	300.91	0.1038	31.600	229.51	0.1031	984.70	1179.1	0.9600	580.00	1.7210	0.5700	**15**
21.000	302.99	0.1273	34.700	231.16	0.1261	1989.8	1185.0	0.9800	620.00	1.8050	0.6190	**16**
23.000	304.33	0.1465	37.300	232.25	0.1446	4000.0	1205.7	0.9900	680.00	1.9070	0.6640	**17**
24.600	305.47	0.1661	39.900	233.30	0.1647	-	-	-	710.00	2.0010	0.6920	**18**
25.900	306.32	0.1835	42.360	234.09	0.1829	-	-	-	740.00	2.0660	0.7160	**19**
27.700	307.14	0.2028	45.080	234.92	0.2026	-	-	-	760.00	2.1600	0.7440	**20**
31.000	308.80	0.2487	52.000	236.53	0.2494	-	-	-	820.00	2.3170	0.7690	**21**
36.000	310.30	0.3031	60.300	238.01	0.3033	-	-	-	900.00	2.5200	0.7930	**22**
42.400	311.44	0.3542	62.000	239.19	0.3543	-	-	-	1100.0	2.7980	0.8210	**23**
48.040	312.30	0.3996	64.000	240.11	0.4005	-	-	-	1300.0	3.1310	0.8280	**24**
55.600	313.13	0.4498	74.000	241.02	0.4505	-	-	-	1800.0	3.7020	0.8520	**25**
64.050	313.83	0.4999	83.960	241.86	0.5008	-	-	-	2300.0	4.3580	0.8590	**26**
74.400	314.46	0.5497	96.770	242.66	0.5509	-	-	-	2650.0	4.7670	0.8690	**27**
84.800	315.04	0.5999	112.42	243.42	0.6010	-	-	-	3200.0	5.3940	0.8720	**28**
103.60	315.60	0.6499	132.35	244.22	0.6509	-	-	-	3940.0	6.0950	0.8790	**29**
122.50	316.17	0.6998	156.54	245.05	0.7012	-	-	-	5010.0	6.5380	0.8820	**30**
1601.0	316.66	0.7398	189.27	245.76	0.7412	-	-	-	7340.0	6.9880	0.9030	**31**
169.50	317.06	0.7700	224.75	246.40	0.7697	-	-	-	8100.0	7.0020	0.9380	**32**
197.80	317.51	0.7999	256.15	247.07	0.8004	-	-	-	8400.0	7.0330	0.9690	**33**
226.06	317.89	0.8199	301.69	247.60	0.8196	-	-	-	9000.0	7.1730	0.9970	**34**
254.30	318.27	0.8401	337.27	248.27	0.8400	-	-	-	-	-	-	**35**
292.00	318.68	0.8599	385.66	249.03	0.8599	-	-	-	-	-	-	**36**
329.00	319.06	0.8749	445.40	249.73	0.8749	-	-	-	-	-	-	**37**
381.50	319.51	0.8900	502.35	250.55	0.8899	-	-	-	-	-	-	**38**
442.70	320.01	0.9049	576.35	251.55	0.9047	-	-	-	-	-	-	**39**
571.70	320.86	0.9252	671.69	253.53	0.9251	-	-	-	-	-	-	**40**
821.00	322.21	0.9469	863.81	256.88	0.9472	-	-	-	-	-	-	**41**
1213.2	323.78	0.9640	1821.5	261.64	0.9638	-	-	-	-	-	-	**42**
2409.4	326.81	0.9817	3875.1	272.39	0.9828	-	-	-	-	-	-	**43**
12000	334.87	0.9963	10000	282.38	0.9933	-	-	-	-	-	-	**44**

Citation: Arjmandi M, Ahmadpour A, Arjmandi A. A new approach for determination of adsorption energy for each adsorption site and improve conventional adsorption isotherms. *Int J Petrochem Sci Eng.* 2018;3(5):131–142. DOI: 10.15406/ipcse.2018.03.00087

Table 5 The fitted Gaussian functions to PSD data and their constants

No.	Gaussian function	constants			
Case 1	$y = a_1 . \exp\left[-\left(\frac{x-b_1}{c_1}\right)^2\right] + ... + a_7 . \exp\left[-\left(\frac{x-b_7}{c_7}\right)^2\right]$	a_1= 0.9239	a_2= -0.2239	a^3= 0.6935	a^4= 0.3112
		a_5= 0.5566	a_6= 5.4910	a^7= 1.0220	b^1= 0.2093
		b_2= 0.2389	b_3= 3.3040	b^4= 2.7050	b^5= 3.4850
		b_6= -0.7398	b_7= 2.6100	c^1= 0.1447	c^2= 0.0857
		c_3= 0.3993	c_4= 0.3227	c^5= 2.7760	c^6= 0.9961
		c_7= 1.2610			
Case 2	$y = a_1 . \exp\left[-\left(\frac{x-b_1}{c_1}\right)^2\right] + ... + a_6 . \exp\left[-\left(\frac{x-b_6}{c_6}\right)^2\right]$	a^1= 0.3481	a_2= 0.2053	a_3= -0.1083	a_4= 0.0470
		a^5= -0.1226	a_6= 1.6030	a_7= 0.0000	b_1= 0.4716
		b^2= 0.1660	b_3= 0.2883	b_4= 0.0757	b_5= 0.2607
		b^6= -0.0510	b_7= 0.0000	c_1= 1.5740	c_2= 0.0625
		c^3= 0.0372	c_4= 0.0422	c_5= 0.0082	c_6= 0.4606
		c^7= 0.0000			
Case 3	$y = a_1 . \exp\left[-\left(\frac{x-b_1}{c_1}\right)^2\right] + ... + a_7 . \exp\left[-\left(\frac{x-b_7}{c_7}\right)^2\right]$	a_1= 0.9380	a_2= 1.1580	a_3= 0.5029	a_4= 0.0519
		a_5= 1.1820	a_6= 1.2510	a_7= -0.1567	b_1= 0.0510
		b_2= 0.0581	b_3= 0.0465	b_4= 0.0673	b_5= 0.0672
		b_6= 0.0413	b_7= 0.1236	c_1= 0.0055	c_2= 0.0089
		c_3= 0.0041	c_4= 0.0026	c_5= 0.0225	c_6= 0.1040
		c_7= 0.0379			
Case 4	$y = a_1 . \exp\left[-\left(\frac{x-b_1}{c_1}\right)^2\right] + ... + a_5 . \exp\left[-\left(\frac{x-b_5}{c_5}\right)^2\right]$	a_1= 0.1970	a_2= 0.2677	a_3= 0.1071	a_4= 0.1832
		a_5= 0.1506	a_6= 0.0000	a_7= 0.0000	b_1= 0.0473
		b_2= 0.0545	b_3= 0.0831	b_4= -0.2019	b_5= 0.0527
		b_6= 0.0000	b_7= 0.0000	c_1= 0.0051	c_2= 0.0092
		c_3= 0.0254	c_4= 0.2520	c_5= 0.0359	c_6= 0.0000
		c_7= 0.0000			

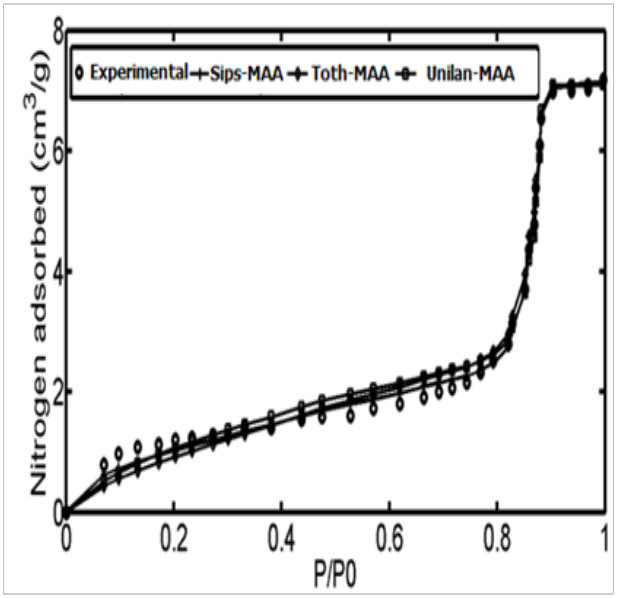

Figure 6 Comparison of experimental data with three modified isotherms; Sips- M.A.A, Unilan- M.A.A and Toth- M.A.A.

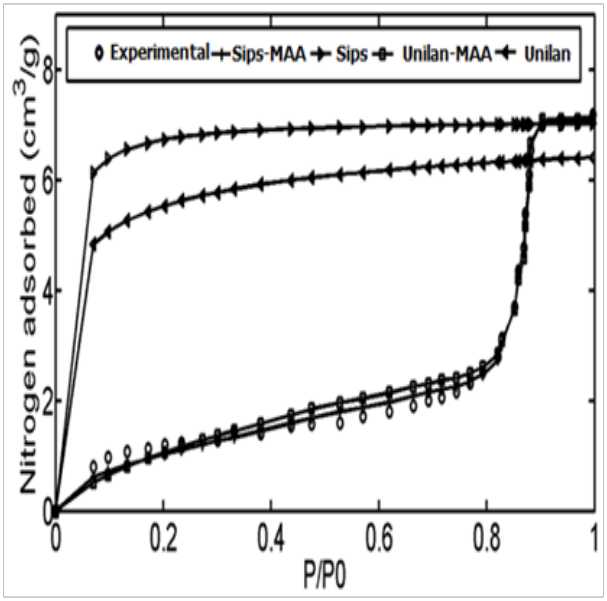

Figure 7 Comparison of experimental data with modified & unmodified isotherms; Sips, Sips- M.A.A , Unilan, Unilan- M.A.A.

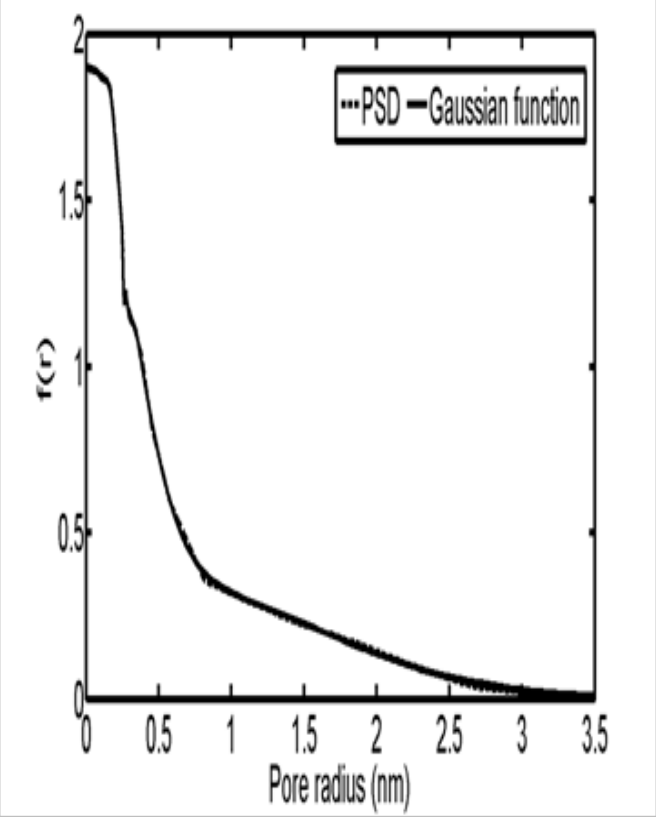

Figure 8 Pore size distribution and fitted Gaussian for NS-$ZnCl_2$.

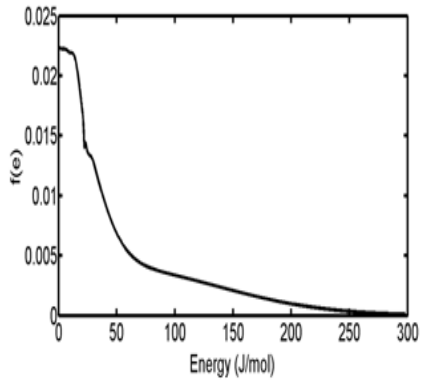

Figure 9 Energy distribution of NS-$ZnCl_2$.

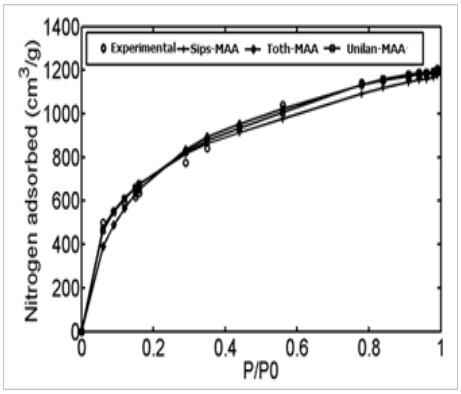

Figure 10 Comparison of experimental data with isotherm models; Sips-NA, Unilan-NA and Toth-NA.

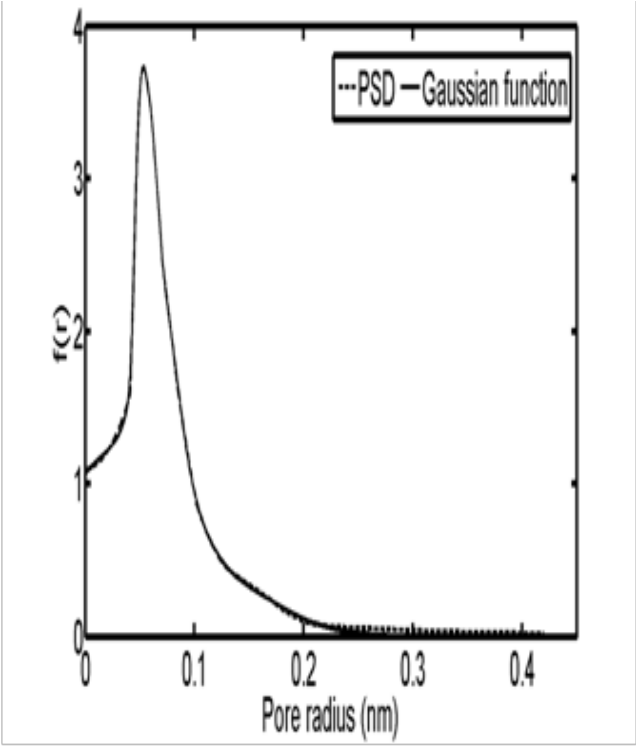

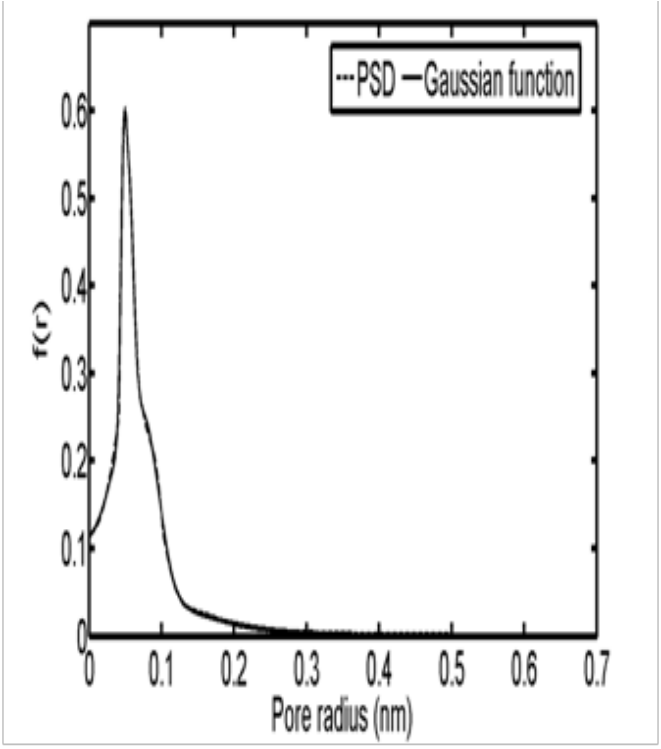

Figure 11 Pore size distribution and the fitted Gaussian functions for; (A) Coal-KOH and (B) NS – KOH.

Citation: Arjmandi M, Ahmadpour A, Arjmandi A. A new approach for determination of adsorption energy for each adsorption site and improve conventional adsorption isotherms. *Int J Petrochem Sci Eng.* 2018;3(5):131–142. DOI: 10.15406/ipcse.2018.03.00087

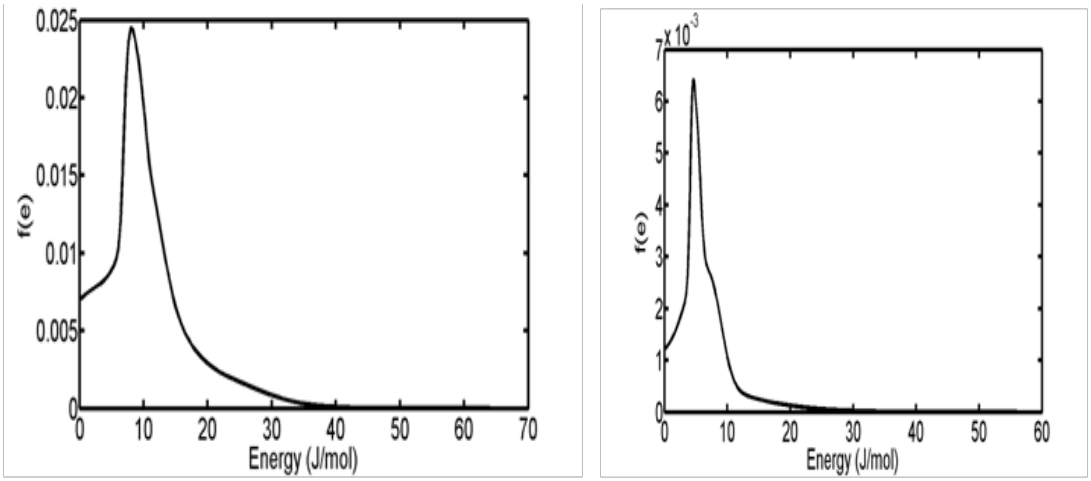

Figure 12 Energy distribution of (A) Coal-KOH and (B) NS - KOH Obtained from f(e).de = f(r).dr equation.

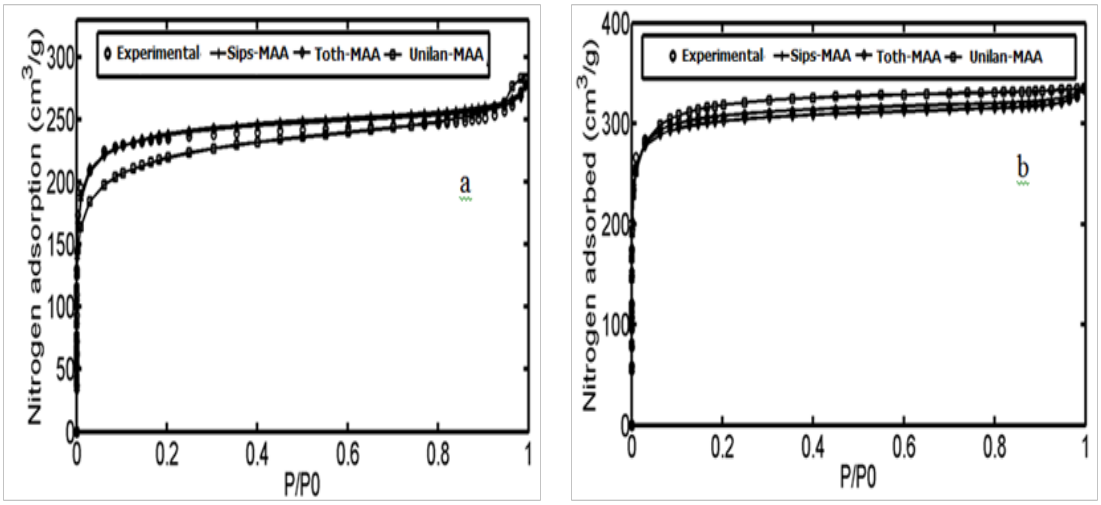

Figure 13 Comparison of experimental data with isotherm; Sips-NA, Unilan-NA, Toth-NA for; (A) Coal-KOH and (B) NS – KOH.

In this study, a new approach for determination of energy distribution (ED) of heterogeneous adsorption systems based on the Kelvin theory of adsorption is presented. The proposed algorithm provides a procedure for reliably estimation of ED of heterogeneous adsorbents from pore size distribution (PSD) data. Moreover, following the presented approach make it possible to estimate the adsorption isotherm accurately. The advantage of the proposed algorithm is that by following such procedure it is possible to evaluate an energy related to solid pores and subsequently determine the amount adsorbed on each solid site with the identified energy. In this algorithm, the PSD of adsorbent is first determined by the method proposed by Shahsavand,[26] and then by considering some assumptions (that are discussed in the theory section) and following the presented algorithm, the ED was determined.

In order to evaluate the proposed algorithm, adsorption data of four different heterogeneous cases were used for estimation of the PSD and subsequently the ED. From the results, the proposed algorithm provided better estimation of adsorption isotherms in all of the investigated cases than conventional adsorption models such as Unilan, Toth and Sips as well as good ED. The accuracy of the proposed approach is greatly depends on the accuracy of the PSD determination method; however, it could be safely applied as reliable procedure for determination of the ED of heterogeneous adsorption systems.[53] On the other hand it seems that the proposed algorithm is benchmark for comparing the accuracy of different methods for calculating the PSD. Because, if the PSD achieved in the first step is not sufficiently accurate ultimately isotherms obtained will be much difference with the experimental data. This entry is being studied and will be reported in subsequent studies.[54]

Acknowledgements

None.

Conflict of interest

The author declares that there is no conflict of interest.

References

1. Do DD. *Performance of an Activated Carbon-Ammonia Adsorption Refrigeration System*. UK: Imperial College Press; 1998. 8 p.

2. Jaroniec M, Madey R. *Physical Adsorption on Heterogeneous Solids*.

Newyork: Elsevier Science Publishers; 1988. 353 p.

3. Rudziński W, Everett DH. *Adsorption of gases on heterogeneous surfaces.* London: Academic Press; 1992. 578 p.
4. Foo KY. Hameed BH. Improvement of Fe(Ii)-Adsorption Capacity of Feooh-Coated Brick in Solutions, and Kinetics Aspects. *Chemical Engineering Journal*. 2010;156(1):2–10.
5. Langmuir I. The Adsorption of Gases on Plane Surfaces of Glass, Mica And Platinum. *J Am Chem Soc*. 1916;40(9):1361–1403.
6. Bruanuer S, Emmett PH. and Teller, E. Adsorption of Gases in Multimolecular Layer. *J. Am. Chem. Soc*. 1938;60:309–319.
7. Bear J. An Integrated Rock Typing Approach for Unraveling the Reservoir Heterogeneity of Tight Sands in the Whicher Range Field of Perth Basin, Western Australia. *American Elsevier Publishing Company*. 1972;4(8):764.
8. Uchida T. Petrophysical Properties of Natural Gas Hydrates-Bearing Sands and Their Sedimentology in the Nankai Trough. *J Jpn Assoc Petrol Technol*. 1987;52(1):79–87.
9. Rudziński W, Jaroniec M. Adsorption on heterogeneous surfaces: A new method for evaluating the energy distribution function. *Surface Science.*1973;42(2):552–564.
10. Gunay A, Arslankaya E. Tosun I. Lead removal from aqueous solution by natural and pretreated clinoptilolite: adsorption equilibrium and kinetics. *J Hazard Mater*. 2007;146:362–371.
11. Russell BP, Levan MD. Pore Size Distribution of BPL Activated Carbon Determined by Different Methods. *Carbon*. 1994;32(5):845–855.
12. De Boer JH. *Dynamical Character of Adsorption*. London: Oxford University Press; 1968.
13. Tarazona P, Marconi UMB, Evans R. Phase equilibria of fluid interfaces and confined fluids Non-local versus local density functional. *Mol Phys.*1987;60(3):573–595.
14. Merz PH. Molecular Dynamics at a Constant pH. *J Comput Phys*. 1980;8(1):47–53.
15. House WA, Jaroniec M, Brauer P, et al. Studies of the surface heterogeneity of high disperse silica chemically modified by sodium and potassium oxides using low-temperature nitrogen adsorption data. *Journal of colloid and interface science*. 1982;99(2):493–506.
16. Duda JT, Duda JT. Kwiatkowski M. Evaluation of adsorption energy distribution of microporous materials by a multivariant identification. *Applied Surface Science.* 2005;252:570–581.
17. Barrett EP, Joyner LG, Halenda PP. The Determination of Pore Volume and Area Distributions in Porous Substances. I. Computations from Nitrogen Isotherms. *J Am Chem Soc*. 1951;73:373–980.
18. Kruk M, Jaroniec M, Sayari A. Application of Large Pore MCM-41 Molecular Sieves To Improve Pore Size Analysis Using Nitrogen Adsorption Measurements. *Langmuir.* 1997;13(23):6267–6273.
19. Horvath G, Kawazoe K. Method for the Calculation of Effective Pore Size Distribution in Molecular Sieve Carbon. *J Chem Eng Jpn*. 1983;16:470–475.
20. Nguyen C, Do DD. Characterizing the Micropore Size Distribution of Activated Carbon Using Equilibrium Data of Many Adsorbates at Various Temperatures. *Langmuir*. 1999;15(23):3608–3633.
21. Kaneko K. Determination of pore size and pore size distribution: 1. Adsorbents and catalysts. *Journal of Membrane Science.* 1994;96(1-2):59–89.
22. Emmanuel S, Ague JJ, Walderhaug O. Interfacial energy effects and the evolution of pore size distributions during quartz precipitation in sandstone. *Geochimica et Cosmochimica Acta*. 2010;74:3539–3552.
23. Gauden PA, Terzyk AP, Kowalczyk P. Some remarks on the calculation of the pore size distribution function of activated carbons**.** *Journal of Colloid and Interface Science*. 2006;300(2):453.
24. Bhattacharya S, Gubbins KE. Fast Method for Computing Pore Size Distributions of Model Materials. *Langmuir*. 2006;22:7726–7731.
25. Gauden PA, Terzyk AP, Jaroniec M. et al. Bimodal pore size distributions for carbons: experimental results and computational studies. *Journal of Colloid and Interface Science*. 2007;310:205.
26. Shahsavand A, Niknam Shahrak M. Direct pore size distribution estimation of heterogeneous nano-structured solid adsorbents from condensation data: Condensation with no prior adsorption. *Colloids and Surfaces A.* 2011;378(1-3):1–13.
27. Shahsavand A, Niknam Shahrak M. Reliable prediction of pore size distribution for nano-sized adsorbents with minimum information requirements. *Chemical Engineering Journal.* 2011;171(1):69–80.
28. Quinones I, Stanley B, Guiochon G. Estimation of the adsorption energy distributions for the Jovanovic–Freundlich isotherm model with Jovanovic local behavior. *Journal of Chromatography* A. 1999;849(1):45–60.
29. Calleja G, Coto B, Morales Cas AM. Adsorption energy distribution in activated carbon from grand canonical Monte Carlo calculation. *Applied Surface Science*. 2006;252(12):4345–4352.
30. Cascarini de Torre LE, Bottani EJ. Colloids and Surfaces A: Physicochemical and Engineering Aspects. *Colloids and Surfaces*. 1996;116:285–291.
31. Papirer E, Li S, Balard H, et al. Chemical modifications and surface properties of carbon blacks. *Carbon*. 1991;29(12):1521–1529.
32. Savard S, Pand Lasia A. Role of Proton-Coupled Electron Transfer in O–O Bond Activation. *Journal of Electroanalytical Chemistry.* 2004;574(7):41–53.
33. Malek A, Farooq S. Comparison of isotherm models for hydrocarbon adsorption on activated carbon. *AIChEJ*. 1996;42(11):3191–3201.
34. Do DD, Nguyen C. Do HD. Characterization of micro-mesoporous carbon media. *Colloids and Surfaces A*. 2001;187:51–71.
35. Myers AL, Prausnitz JM. Thermodynamics of mixed-gas adsorption. *AIChE J.* 1965;11(1):121–127.
36. Dubinin MM. The Potential Theory of Adsorption of Gases and Vapors for Adsorbents with Energetically Nonuniform Surfaces. *Chem. Rev*. 1960;60(2):235–241.
37. Freundlich HMF. Kinetics and Thermodynamics of Adsorption Methylene Blue onto Tea Waste/CuFe2O4 Composite. *J Phys Chem*. 1906;57:385–471.
38. Altin O, Ozbelge HO, Dogu T. Use of General Purpose Adsorption Isotherms for Heavy Metal–Clay Mineral Interactions. *J Colloid Interface Sci.* 1998;198(1):130–140.
39. Vijayaraghavan K, Padmesh TVN, Palanivelu K, et al. Biosorption of nickel(II) ions onto Sargassum wightii: application of two-parameter and three-parameter isotherm models. *J Hazard Mater*. 2006;133(1-3):304–308.
40. William H. *Numerical Recipes in C: The Art of Scientific Computing*. 2nd ed. UK: Cambridge University Press; 1992. 1018 p.
41. Szombathely MV, Brauer P, Jaroniec M. The solution of adsorption integral equations by means of the regularization method. *Journal of Computational Chemistry.*1992;13(1):17–32.

42. Venkatesh PK. Specificity of MAPK signaling towards FLO11 expression is established by crosstalk from cAMP pathway. *Physical A*. 2000;284(2):448–418.

43. Ahmadian H, Mottershead JE, Friswell MI. Regularisation methods for finite element model updating. *Mechanical Systems and Signal* Processing.1998;12(1):47–64.

44. Yagola A, Titarenko V. *Moscow State University Moscow* 119899. Russia: 2000.

45. Yeun YS, Lee KH, Han SM, et al. Fuzzy filters of MTL-algebras. *Information Sciences.*2001;133(1-2):120–138.

46. Shahsavand A. Thesis. UK: University of Surrey; 2000.

47. Rouquerol F, Rouquerol J, Sing K. *Adsorption by Powders and Porous Solids.* London: Academic Press; 1999. 467 p.

48. Solcova O, Matêjová L, Schneider P. Pore-size distributions from nitrogen adsorption revisited: Models comparison with controlled-pore glasses. *Applied Catalysis A*. 2006;313(2):167–176.

49. Ahmadpour A, King B, Do DD. Comparison of Equilibria and Kinetics of High Surface Area Activated Carbon Produced from Different Precursors and by Different Chemical Treatments. *Ind Eng Chem Res*. 1998;37:1329–1334.

50. Ahmadpour A, Do DD. The preparation of activated carbon from macadamia nutshell by chemical activation *Carbon*. 1997;35:1723–1732.

51. Toth J. *Acta Chem Acad Hung.* 1979;69:311.

52. Sips R. The Structure of a Catalyst Surface. *J Chem Phys.*1948;16:490–495.

53. Sidney D. Pore size distributions in clays. *Clays and Clay Minerals*. 1970;18:7–23.

54. Zarzycki P. Effective adsorption energy distribution functions as a new mean-field characteristic of surface heterogeneity in adsorption systems with lateral interactions. *Journal of Colloid and Interface Science*. 2007;311(2):622–627.

Citation: Arjmandi M, Ahmadpour A, Arjmandi A. A new approach for determination of adsorption energy for each adsorption site and improve conventional adsorption isotherms. *Int J Petrochem Sci Eng.* 2018;3(5):131–142. DOI: 10.15406/ipcse.2018.03.00087